

# Flavor Evolution of the Neutronization Neutrino Burst from an O-Ne-Mg Core-Collapse Supernova

Huaiyu Duan,<sup>1</sup> George M. Fuller,<sup>2,1</sup> J. Carlson,<sup>3</sup> and Yong-Zhong Qian<sup>4</sup>

<sup>1</sup>*Institute for Nuclear Theory, University of Washington, Seattle, WA 98195*

<sup>2</sup>*Department of Physics, University of California, San Diego, La Jolla, CA 92093*

<sup>3</sup>*Theoretical Division, Los Alamos National Laboratory, Los Alamos, NM 87545*

<sup>4</sup>*School of Physics and Astronomy, University of Minnesota, Minneapolis, MN 55455*

We present results of 3-neutrino flavor evolution simulations for the neutronization burst from an O-Ne-Mg core-collapse supernova. We find that nonlinear neutrino self-coupling engineers a single spectral feature of stepwise conversion in the inverted neutrino mass hierarchy case and in the normal mass hierarchy case, a superposition of two such features corresponding to the vacuum neutrino mass-squared differences associated with solar and atmospheric neutrino oscillations. These neutrino spectral features offer a unique potential probe of the conditions in the supernova environment and may allow us to distinguish between O-Ne-Mg and Fe core-collapse supernovae.

PACS numbers: 14.60.Pq, 97.60.Bw

In this Letter we suggest an exciting new neutrino signal-based probe of conditions deep inside a supernova. We do this by performing the first fully self-coupled 3-neutrino flavor ( $3 \times 3$ ) evolution calculations. Stars of  $\sim 8\text{--}11 M_\odot$  develop degenerate O-Ne-Mg cores, at least some of which eventually collapse to produce supernovae (e.g., Refs. [1, 2, 3]). The matter density falls off so steeply in the region between such a core and the hydrogen envelope that there is little hindrance to the outgoing supernova shock. Consequently, O-Ne-Mg core-collapse supernovae are the only case where neutrino-driven explosion has been demonstrated by several groups [4, 5, 6]. Such supernovae may be the site for producing the heaviest elements by rapid neutron capture [7] and may also explain the observed subluminescent supernovae [5]. They are expected to be relatively common because the known progenitors of most core-collapse supernovae lie in the mass range  $\sim 8\text{--}20 M_\odot$  (e.g., Ref. [8]).

The region of steeply-falling matter density immediately above an O-Ne-Mg core provides an extremely interesting environment for studying neutrino flavor evolution. For the vacuum neutrino mass-squared differences  $\Delta m_{\text{atm}}^2$  and  $\Delta m_\odot^2$  associated with atmospheric and solar neutrino oscillations, respectively, the two corresponding conventional Mikheyev-Smirnov-Wolfenstein (MSW) [9, 10] resonances occur with very small radial separation in this region. As the neutrino number density decreases much more gently with radius than the matter density, neutrino self-coupling can affect flavor evolution associated with both  $\Delta m_{\text{atm}}^2$  and  $\Delta m_\odot^2$ , and a full treatment of  $3 \times 3$  mixing appears to be required. To identify clearly any new physics, we study the relatively simple case of the neutronization burst, which consists of predominantly  $\nu_e$  emitted when the shock breaks through the neutrino sphere.

Traditional analyses of flavor evolution of supernova neutrinos are based on the pure matter-driven MSW effect (see, e.g., Refs. [11, 12, 13, 14]). The evolution of

neutrino flavor state  $|\psi\rangle$  in matter is described by the Schrödinger-like equation,

$$i \frac{d}{dt} |\psi\rangle = \hat{H} |\psi\rangle, \quad (1)$$

where  $t$  is an Affine parameter along the neutrino worldline, and the Hamiltonian  $\hat{H}$  is composed of two pieces:  $\hat{H} = \hat{H}_{\text{vac}} + \hat{H}_{\text{matt}}$ . The matter contribution is  $\langle \nu_\alpha | \hat{H}_{\text{matt}} | \nu_\beta \rangle = \sqrt{2} G_F n_e \delta_{\alpha\beta} \delta_{e\alpha}$ , where  $G_F$  is the Fermi constant,  $n_e$  is the electron number density, and  $|\nu_\alpha\rangle$  denotes a pure flavor state with  $\alpha = e, \mu, \tau$ . The vacuum piece of  $\hat{H}$  is  $\langle \nu_\alpha | \hat{H}_{\text{vac}} | \nu_\beta \rangle = (2E_\nu)^{-1} (U M U^\dagger)_{\alpha\beta}$ , where  $E_\nu$  is the neutrino energy. The transformation  $U_{\alpha i}$  relates pure flavor state  $|\nu_\alpha\rangle$  to vacuum mass eigenstate  $|\nu_i\rangle$  (see Chap. 13 of Ref. [15] for our convention):  $|\nu_\alpha\rangle = \sum_{i=1,2,3} U_{\alpha i}^* |\nu_i\rangle$ . The mass matrix is diagonal in the vacuum mass basis,  $M = \text{diag}(0, \Delta m_{21}^2, \Delta m_{21}^2 + \Delta m_{32}^2)$ , where the mass-squared differences are  $\Delta m_{ij}^2 = m_i^2 - m_j^2$ . In calculations presented here we take the three mixing angles and the CP violating phase to be  $\theta_{12} = 0.6$ ,  $\theta_{23} = \pi/4$ ,  $\theta_{13} = 0.1$ ,  $\delta = 0$ , respectively. We take  $\Delta m_{21}^2 = 8 \times 10^{-5} \text{ eV}^2 \simeq \Delta m_\odot^2$  and  $\Delta m_{32}^2 = \pm 3 \times 10^{-3} \text{ eV}^2 \simeq \pm \Delta m_{\text{atm}}^2$ , where the plus (minus) sign is for the normal (inverted) mass hierarchy.

In pure matter-driven MSW evolution, for small  $\theta_{13}$ , the  $\nu_e$  survival probability  $P_{\nu_e \nu_e} = |\langle \nu_e | \psi \rangle|^2$  can be factorized [11]:  $P_{\nu_e \nu_e} = P_{\nu_e \nu_e}^H P_{\nu_e \nu_e}^L$ , where  $P_{\nu_e \nu_e}^H$  and  $P_{\nu_e \nu_e}^L$  are the  $\nu_e$  survival probabilities in 2-flavor ( $2 \times 2$ ) mixing processes at the  $\Delta m_{\text{atm}}^2$  and  $\Delta m_\odot^2$  scales, respectively. In other words, the full  $3 \times 3$  MSW result is the superposition of two independent  $2 \times 2$  MSW scenarios, one for each of the solar and atmospheric mass-squared differences.

Using the  $n_e$  profile for the O-Ne-Mg core model of Refs. [1, 2] and the neutrino mixing parameters given above, we show  $P_{\nu_e \nu_e}$  as a function of  $E_\nu$  in Fig. 1 assuming pure matter-driven MSW evolution. The results shown are for radius  $r = 5000 \text{ km}$ , where the vacuum Hamiltonian dominates for most neutrino energies. The

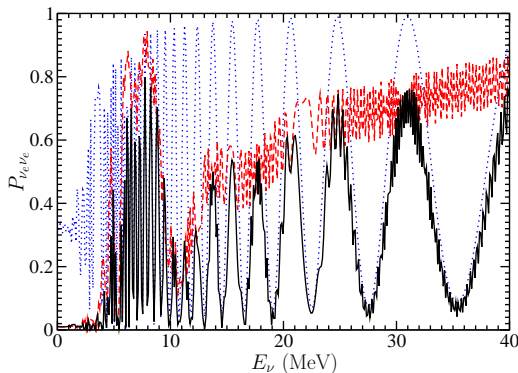


FIG. 1: (Color online) Neutrino survival probabilities  $P_{\nu_e \nu_e}$  as functions of neutrino energy  $E_\nu$  for pure matter-driven MSW evolution. The  $2 \times 2$  flavor mixing cases with  $\Delta m^2 \simeq \Delta m_{\text{atm}}^2$  and  $\Delta m_{\odot}^2$  are shown as the dashed and dotted lines, respectively. The  $2 \times 2$  flavor mixing case with  $\Delta m^2 \simeq -\Delta m_{\text{atm}}^2$  (not shown) corresponds to  $P_{\nu_e \nu_e} \simeq 1$  for all energies. The solid line gives  $P_{\nu_e \nu_e}(E_\nu)$  for full  $3 \times 3$  flavor mixing with the normal mass hierarchy. The  $3 \times 3$  inverted mass hierarchy case (not shown) is almost identical to the dotted line.

dashed and dotted lines in this figure show the  $2 \times 2$  flavor mixing cases with the normal mass hierarchy for  $\Delta m^2 = 3 \times 10^{-3} \text{eV}^2$  ( $\simeq \Delta m_{\text{atm}}^2$ ) and  $8 \times 10^{-5} \text{eV}^2$  ( $\simeq \Delta m_{\odot}^2$ ), respectively. In these cases we take the effective  $2 \times 2$  vacuum mixing angles to be  $\theta = 0.1$  and  $0.6$ , respectively. We note that in either case MSW flavor transformation for neutronization burst neutrinos of average energy  $\langle E_{\nu_e} \rangle = 11$  MeV is neither fully adiabatic ( $P_{\nu_e \nu_e} = \sin^2 \theta$ ) nor fully non-adiabatic ( $P_{\nu_e \nu_e} = \cos^2 \theta$ ) due to the rapid decrease of matter density  $\rho$  with radius in the region of interest ( $|\text{d}(\ln \rho)/\text{d}r| \gtrsim 0.04 \text{km}^{-1}$ ). The spike in  $P_{\nu_e \nu_e}^{\text{H}}(E_\nu)$  (dashed line) at  $E_\nu \simeq 8$  MeV is caused by a sharp change in  $n_e$  at the base of the hydrogen envelope, where the electron fraction  $Y_e$  jumps from 0.5 to  $\sim 0.85$ . The  $2 \times 2$  inverted mass hierarchy case with  $\Delta m^2 \simeq -\Delta m_{\text{atm}}^2$  has  $P_{\nu_e \nu_e} \simeq 1$  for all energies (i.e., no MSW resonance). In the complete  $3 \times 3$  mixing case with the normal mass hierarchy,  $P_{\nu_e \nu_e}$  is given by the solid line. This case corresponds closely to a succession of two independent  $2 \times 2$  mixing schemes, with the solid line being approximated by the product of the values of the dashed ( $P_{\nu_e \nu_e}^{\text{H}}$ ) and dotted ( $P_{\nu_e \nu_e}^{\text{L}}$ ) lines. The  $3 \times 3$  inverted mass hierarchy case gives  $P_{\nu_e \nu_e}$  nearly identical to the dotted line.

In supernovae, where neutrino luminosities are large, neutrino-neutrino forward scattering contributes another term for the Hamiltonian [16, 17, 18]

$$\hat{H}_{\nu\nu} = \sqrt{2}G_{\text{F}} \sum_{\lambda} n_{\nu,\lambda} |\psi_{\lambda}\rangle \langle \psi_{\lambda}|, \quad (2)$$

where  $\sum_{\lambda}$  sums over all background neutrino states  $|\psi_{\lambda}\rangle$  with number density  $n_{\nu,\lambda}$ . To simplify the problem, we adopt the “single-angle approximation” in which neutri-

nos emitted in all directions from the neutrino sphere have the same flavor evolution histories as those with the same energies but propagating along a radial trajectory. With this approximation we have

$$\sum_{\lambda} n_{\nu,\lambda} \longrightarrow \frac{D(r/R_{\nu})}{2\pi R_{\nu}^2} \frac{L_{\nu_e}}{\langle E_{\nu_e} \rangle} \int \text{d}E_{\nu} f_{\nu_e}(E_{\nu}), \quad (3)$$

where  $D(\xi) = \frac{1}{2}(1 - \sqrt{1 - \xi^{-2}})^2$ . In our calculations for the neutronization burst we assume  $\nu_e$  is the only neutrino species emitted from the neutrino sphere (at radius  $R_{\nu} = 60$  km) and take the  $\nu_e$  luminosity to be  $L_{\nu_e} = 10^{53}$  erg/s. The  $\nu_e$  energy distribution function  $f_{\nu_e}(E_{\nu})$  is taken to be of Fermi-Dirac form with degeneracy parameter  $\eta = 3$  and with an average  $\nu_e$  energy  $\langle E_{\nu_e} \rangle = 11$  MeV. Full  $2 \times 2$  multi-angle simulations show that the single-angle approximation appears to be adequate for qualitative studies of the collective flavor transformation phenomena of interest here [19, 20, 21].

Fig. 2 shows the results of single-angle simulations of full  $3 \times 3$  neutrino flavor evolution including nonlinear neutrino self-coupling for the neutrino mixing and emission parameters given above. Results for both the inverted (upper panels) and normal (lower panels) neutrino mass hierarchies are presented, again at radius  $r = 5000$  km as in Fig. 1. The left-hand panels show the probability  $|a_{\nu_i}|^2 = |\langle \nu_i | \psi \rangle|^2$  for neutrinos to be in each of the mass eigenstates  $|\nu_i\rangle$ , and the right-hand panels show the probability  $|a_{\nu_{\alpha}}|^2 = |\langle \nu_{\alpha} | \psi \rangle|^2$  for neutrinos to be in each of the flavor states  $|\nu_{\alpha}\rangle$ .

The inverted neutrino mass hierarchy produces a stepwise  $\nu_2/\nu_1$  conversion at energy  $E_{\nu} \simeq 11$  MeV [Fig. 2(a)]. This spectral swap feature can be understood in a  $2 \times 2$  mixing scheme with  $\Delta m^2 \simeq \Delta m_{\odot}^2$  (see, e.g., Ref. [22]). In this scheme the flavor evolution of a neutrino can be represented as the precession of a spin or polarization vector in flavor isospace, in analogy to a magnetic spin (e.g., Ref. [18]). When neutrino number fluxes are large, the neutrino self-coupling is strong and the “magnetic spins” representing neutrinos can rotate collectively in the region where a neutrino with a representative energy would experience a resonance in the pure matter-drive MSW evolution [23]. This corresponds to a neutrino-background-enhanced MSW-like flavor transformation [22, 23, 24, 25]. Subsequently, the “magnetic spins” will enter a collective precession mode. As neutrino fluxes become small at large radii and the collective precession mode dies out, a mass-basis spectral swap is established [26, 27]. The swap point in the neutrino energy spectrum is determined by conservation of a mass-basis “lepton number” [27, 28]. In fact, the result of the full  $3 \times 3$  calculation agrees very well with that of the  $2 \times 2$  calculation with  $\Delta m^2 \simeq \Delta m_{\odot}^2$ . In contrast to the pure-matter driven MSW evolution, neutrinos on the two sides of the swap point appear to have experienced almost fully adiabatic or fully non-adiabatic flavor trans-

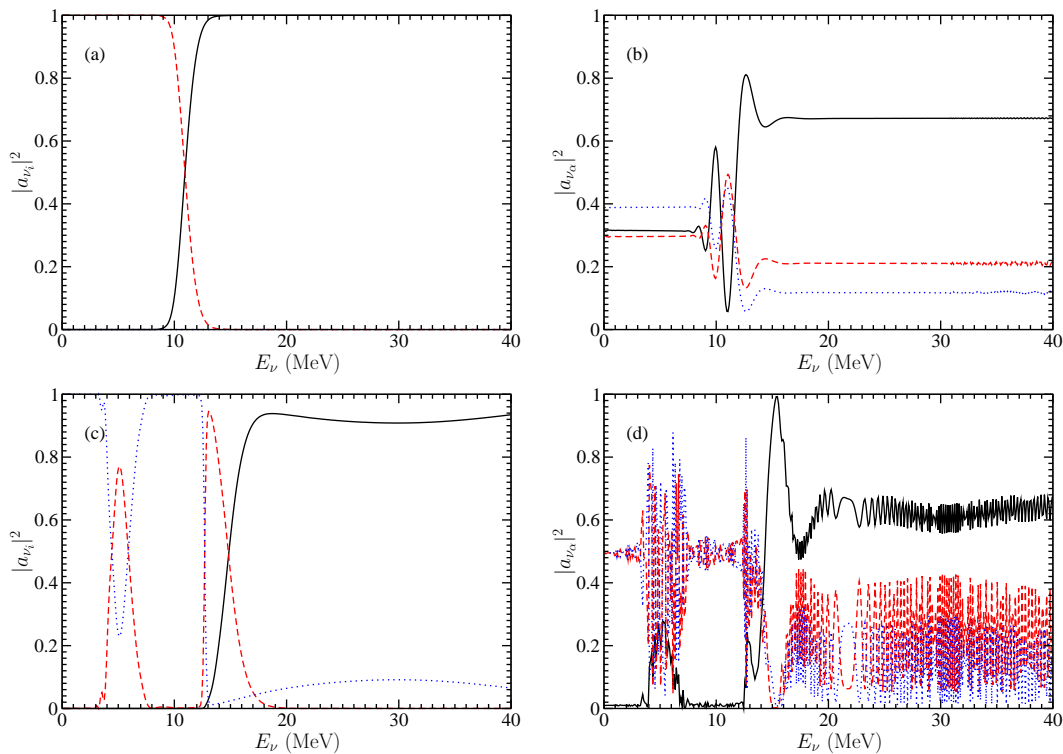


FIG. 2: (Color online) Probabilities as functions of neutrino energy  $E_\nu$  for neutrinos to be in each vacuum mass eigenstate ( $|a_{\nu_i}|^2$ , left panels) and flavor eigenstate ( $|a_{\nu_\alpha}|^2$ , right panels), respectively. The solid, dashed and dotted lines represent the  $\nu_1$ ,  $\nu_2$ , and  $\nu_3$  states in the left panels and the  $\nu_e$ ,  $\nu_\mu$ , and  $\nu_\tau$  states in the right panels. Top (bottom) panels show the inverted (normal) mass hierarchy case.

formation with those in the low (high) mass eigenstate ending up on the right (left) hand side of the swap point. We note that no neutrino-background-enhanced MSW-like flavor transformation occurs at the  $\Delta m_{\text{atm}}^2$  scale in the inverted mass hierarchy case. This is analogous to the pure matter-driven MSW evolution. We also note that conservation of the mass-basis lepton number prohibits the formation of a spectral swap in the corresponding  $2 \times 2$  mixing scheme with  $\Delta m^2 \simeq -\Delta m_{\text{atm}}^2$  because all neutrinos start as  $\nu_e$  in our calculation [38].

Because  $\theta_{12}$  is large,  $P_{\nu_e\nu_e}(E_\nu)$  exhibit a large oscillatory feature in the transition region near the stepwise  $\nu_2/\nu_1$  conversion point at  $E_\nu \sim 11$  MeV [see Fig. 2(b)]. Outside this region, spectral swap can also be seen for the neutrino flavor states. For example,  $P_{\nu_e\nu_e} \simeq |U_{e2}|^2 \simeq 0.32$  ( $|U_{e1}|^2 \simeq 0.67$ ) for  $E_\nu \lesssim 9$  MeV ( $E_\nu \gtrsim 16$  MeV). Note that  $|a_{\nu_\mu}|^2$  is larger (smaller) than  $|a_{\nu_\tau}|^2$  in the energy regime  $E_\nu \gtrsim 13$  MeV ( $E_\nu \lesssim 10$  MeV). This is a consequence of setting the CP-violating phase to  $\delta = 0$ . As  $\delta$  is increased,  $|a_{\nu_\tau}|^2$  increases (decreases) for  $E_\nu \gtrsim 13$  MeV ( $E_\nu \lesssim 10$  MeV), and  $|a_{\nu_\mu}|^2 = |a_{\nu_\tau}|^2$  for  $\delta = \pi/2$ . For  $\delta = \pi$ , the  $|a_{\nu_\mu}|^2$  and  $|a_{\nu_\tau}|^2$  curves in Fig. 2(b) switch places.

Fig. 2(c) shows that the normal neutrino mass hierarchy produces a superposition of two spectral swap fea-

tures, reminiscent of the factorization property of pure matter-driven MSW evolution. The  $\nu_3/\nu_2$  swap at  $E_\nu \simeq 12.7$  MeV and the  $\nu_2/\nu_1$  swap at  $E_\nu \simeq 15$  MeV correspond to those in the  $2 \times 2$  schemes with  $\Delta m^2 \simeq \Delta m_{\text{atm}}^2$  and  $\Delta m_{\odot}^2$ , respectively. This result seems to justify the  $2 \times 2$  approximation used in previous work (e.g., Refs.[19, 20, 21, 23, 25, 29, 30, 31, 32]), but is somewhat surprising given the nonlinear nature of neutrino self-coupling and the fact that the regions of collective flavor transformation for  $\Delta m_{\text{atm}}^2$  and  $\Delta m_{\odot}^2$  overlap with each other. We note that the  $\nu_3/\nu_2$  swap is much sharper than the  $\nu_2/\nu_1$  swap. We also note that the dip (bump) in  $|a_{\nu_3}|^2$  ( $|a_{\nu_2}|^2$ ) centered at  $E_\nu \simeq 5.2$  MeV corresponds to the abrupt change in  $n_e$  at the base of the hydrogen envelope. This feature in the  $n_e$  profile reduces the efficiency of the neutrino-background-enhanced MSW-like transformation of  $\nu_e$  at the  $\Delta m_{\text{atm}}^2$  scale. A similar feature is also present in the pure matter-driven MSW evolution, but in a different energy range (see Fig. 1).

As in the inverted mass hierarchy case, the spectral swaps are also present in the flavor basis [see Fig. 2(d)]. Except for the moderate bump centered at  $E_\nu \simeq 5.2$  MeV, nearly all  $\nu_e$ 's are transformed (with  $P_{\nu_e\nu_e} \simeq |U_{e3}|^2 \simeq 0.01$ ) below the  $\nu_3/\nu_2$  swap energy  $E_\nu \simeq 12.7$  MeV. In contrast, there is less significant  $\nu_e$  depletion

above the  $\nu_2/\nu_1$  swap energy  $E_\nu \simeq 15$  MeV, for which energy range  $P_{\nu_e\nu_e} \simeq |U_{e1}|^2 \simeq 0.67$  would be expected. The bump in  $P_{\nu_e\nu_e}(E_\nu)$  at  $E_\nu \simeq 5.2$  MeV corresponds to the feature in  $|a_{\nu_2}|^2$  at the same energy as explained above. On the other hand, we note that the apparent peak of  $P_{\nu_e\nu_e}(E_\nu)$  in  $E_\nu \simeq 15.5$  MeV is part of the same oscillation feature discussed above for Fig. 2(b). This oscillation feature will disappear at very large distances where coherence has been lost.

The spectral swap features illustrated here for the neutronization burst from an O-Ne-Mg core-collapse supernova are not expected to be present for an Fe-core collapse supernova. This is because at the neutronization burst epoch, there is an extended region of high  $n_e$  above an Fe core. So in this case high neutrino fluxes are always accompanied by high  $n_e$ , which inhibits neutrino-background-enhanced MSW-like flavor transformation. The studies of neutrinos from Fe core-collapse supernovae based on pure matter-driven MSW evolution show that the  $\nu_e$  survival probability is  $P_{\nu_e\nu_e} \simeq \sin^2 \theta_\odot \simeq 0.32$  or less for either mass hierarchy (see, e.g., Table I in Ref. [33]). If enough high-energy ( $E_\nu \gtrsim 15$  MeV) neutrino events are collected from the neutronization burst of a future Galactic supernova in both the charged-current and neutral-current channels, the progenitor may be identified as having an O-Ne-Mg or Fe core based on whether or not  $\nu_e$  is the dominant species in the burst. Because the total neutrino fluence over the  $\sim 10$  ms duration of the neutronization burst is only a small fraction of that emitted during the first several seconds after the onset of core collapse, collection of the required number of events from the neutronization burst may be beyond the capabilities of existing detectors but could be within the reach of proposed megaton water Cherenkov detectors [33, 34, 35] and liquid argon detectors like ICARUS [36, 37]. The low-energy ( $\lesssim 10$  MeV) neutrino signals in the O-Ne-Mg core-collapse supernova neutronization burst, though even more difficult to detect, carry information that potentially can distinguish between the neutrino mass hierarchies [see Figs. 2(b) and (d)].

We thank K. Nomoto for providing the electron number density profile in his O-Ne-Mg core model. We appreciate the hospitality of the Institute for Nuclear Theory at the University of Washington during the completion of this work. This work was supported in part by NSF grant PHY-04-00359 at UCSD, DOE grants DE-FG02-87ER40328 at UMN, DE-FG02-00ER41132 at INT, an IGGP/LANL mini-grant, and by the DOE Office of Nuclear Physics, the LDRD Program and Open Supercomputing at LANL.

---

[1] K. Nomoto, *Astrophys. J.* **277**, 791 (1984).  
 [2] K. Nomoto, *Astrophys. J.* **322**, 206 (1987).

[3] C. Ritossa, E. García-Berro, and I. J. Iben, *Astrophys. J.* **515**, 381 (1999).  
 [4] R. Mayle and J. R. Wilson, *Astrophys. J.* **334**, 909 (1988).  
 [5] F. S. Kitaura, H.-T. Janka, and W. Hillebrandt, *Astron. Astrophys.* **450**, 345 (2006), astro-ph/0512065.  
 [6] L. Dessart et al., *Astrophys. J.* **644**, 1063 (2006), astro-ph/0601603.  
 [7] H. Ning, Y. Z. Qian, and B. S. Meyer, *Astrophys. J.* **667**, L159 (2007), arXiv:0708.1748 [astro-ph].  
 [8] W.-D. Li et al., *Astrophys. J.* **641**, 1060 (2006), astro-ph/0507394.  
 [9] L. Wolfenstein, *Phys. Rev.* **D17**, 2369 (1978).  
 [10] S. P. Mikheyev and A. Y. Smirnov, *Yad. Fiz.* **42**, 1441 (1985), [*Sov. J. Nucl. Phys.* **42**, 913 (1985)].  
 [11] T.-K. Kuo and J. T. Pantaleone, *Phys. Rev.* **D37**, 298 (1988).  
 [12] A. S. Dighe and A. Y. Smirnov, *Phys. Rev.* **D62**, 033007 (2000), hep-ph/9907423.  
 [13] C. Lunardini and A. Y. Smirnov, *JCAP* **0306**, 009 (2003), hep-ph/0302033.  
 [14] J. P. Kneller and G. C. McLaughlin, *Phys. Rev.* **D73**, 056003 (2006), hep-ph/0509356.  
 [15] W.-M. Yao et al., *J. Phys.* **G33**, 1 (2006).  
 [16] G. M. Fuller, R. W. Mayle, J. R. Wilson, and D. N. Schramm, *Astrophys. J.* **322**, 795 (1987).  
 [17] J. T. Pantaleone, *Phys. Rev.* **D46**, 510 (1992).  
 [18] G. Sigl and G. Raffelt, *Nucl. Phys.* **B406**, 423 (1993).  
 [19] H. Duan, G. M. Fuller, J. Carlson, and Y.-Z. Qian, *Phys. Rev.* **D74**, 105014 (2006), astro-ph/0606616.  
 [20] A. Esteban-Pretel, S. Pastor, R. Tomas, G. G. Raffelt, and G. Sigl, *Phys. Rev.* **D76**, 125018 (2007), arXiv:0706.2498 [astro-ph].  
 [21] G. L. Fogli, E. Lisi, A. Marrone, and A. Mirizzi (2007), arXiv:0707.1998 [hep-ph].  
 [22] H. Duan, G. M. Fuller, and Y.-Z. Qian, *Phys. Rev.* **D76**, 085013 (2007), arXiv:0706.4293 [astro-ph].  
 [23] S. Pastor and G. Raffelt, *Phys. Rev. Lett.* **89**, 191101 (2002), astro-ph/0207281.  
 [24] Y. Z. Qian and G. M. Fuller, *Phys. Rev.* **D51**, 1479 (1995), astro-ph/9406073.  
 [25] G. M. Fuller and Y.-Z. Qian, *Phys. Rev.* **D73**, 023004 (2006), astro-ph/0505240.  
 [26] H. Duan, G. M. Fuller, J. Carlson, and Y.-Z. Qian, *Phys. Rev.* **D75**, 125005 (2007), astro-ph/0703776.  
 [27] G. G. Raffelt and A. Y. Smirnov, *Phys. Rev.* **D76**, 081301(R) (2007), arXiv:0705.1830 [hep-ph].  
 [28] S. Hannestad, G. G. Raffelt, G. Sigl, and Y. Y. Wong, *Phys. Rev.* **D74**, 105010 (2006), astro-ph/0608695.  
 [29] A. B. Balantekin and H. Yüksel, *New J. Phys.* **7**, 51 (2005), astro-ph/0411159.  
 [30] H. Duan, G. M. Fuller, and Y.-Z. Qian, *Phys. Rev.* **D74**, 123004 (2006), astro-ph/0511275.  
 [31] H. Duan, G. M. Fuller, J. Carlson, and Y.-Z. Qian, *Phys. Rev. Lett.* **97**, 241101 (2006), astro-ph/0608050.  
 [32] H. Duan, G. M. Fuller, J. Carlson, and Y.-Z. Qian, *Phys. Rev. Lett.* **99**, 241802 (2007), arXiv:0707.0290 [astro-ph].  
 [33] M. Kachelriess et al., *Phys. Rev.* **D71**, 063003 (2005), astro-ph/0412082.  
 [34] Y. Itow et al. (The T2K) (2001), hep-ex/0106019.  
 [35] M. Goodman et al., UNO whitepaper (2001), PREPRINT-SBHEP01-3.  
 [36] I. Gil-Botella and A. Rubbia, *JCAP* **0310**, 009 (2003), hep-ph/0307244.

- [37] C. Vignoli, D. Barni, J. M. Disdier, D. Rampoldi, and G. Passardi (ICARUS), AIP Conf. Proc. **823**, 1643 (2006).
- [38] A. Mirizzi (2007), private communication.